

Analysis and evaluation of the total and partial photoneutron reaction cross sections on ^{94}Zr

V. V. Varlamov,¹ B. S. Ishkhanov,^{2,1} V. N. Orlin,¹ N. N. Peskov,¹ and K. A. Stopani¹

¹*Lomonosov Moscow State University, Skobeltsyn Institute of Nuclear Physics, Moscow, 119991 Russia*

²*Lomonosov Moscow State University, Department of Physics, Moscow, 119991 Russia*

(Dated: July 19, 2015)

Experimental data on photodisintegration of the ^{94}Zr isotope obtained using quasimonoenergetic annihilation photons with neutron multiplicity sorting technique are analyzed. The cross sections of the $(\gamma, 1n)$, $(\gamma, 2n)$, and $(\gamma, 3n)$ reactions are shown to not satisfy the physical reliability criteria. Within the experimentally-theoretical method of evaluation of partial reaction cross sections new data on the partial reaction cross sections and the total photoneutron reaction cross section $(\gamma, \text{tot}) = (\gamma, 1n) + (\gamma, 2n) + (\gamma, 3n) + \dots$ were obtained.

I. INTRODUCTION

Experimental data on photodisintegration of a number of medium and heavy nuclei ($^{90,91}\text{Zr}$, ^{115}In , $^{112,114,116-120,122,124}\text{Sn}$, ^{159}Tb , ^{181}Ta , ^{197}Au) by quasimonoenergetic annihilation photons were analyzed in works [1–6]. It was noticed that the cross sections of the $(\gamma, 1n)$, $(\gamma, 2n)$, and $(\gamma, 3n)$ partial reactions contain systematic errors, which manifest themselves in the behavior of the neutron multiplicity transitional functions

$$F_i = \sigma(\gamma, in)/\sigma(\gamma, Sn) = \sigma(\gamma, in)/\sigma[(\gamma, 1n) + 2(\gamma, 2n) + 3(\gamma, 3n) + \dots]. \quad (1)$$

In certain energy regions F_i exceed the allowed limits $(1, 1/2, 1/3, \dots)$ for, respectively, $i = 1, 2, 3, \dots$. The cross sections of reactions, mainly $(\gamma, 1n)$, often take negative values.

It was shown that the systematic uncertainties of the partial photoneutron reaction cross sections are a result of the employed technique of photoneutron multiplicity discrimination based on the kinetic energy [1–6] and a combined method of evaluation of the of the partial reaction cross sections was proposed [1, 2]. The method makes use of the experimental photoneutron yield cross sections

$$\sigma(\gamma, Sn) \approx \sigma(\gamma, 1n) + 2\sigma(\gamma, 2n) + 3\sigma(\gamma, 3n) + \dots, \quad (2)$$

which do not depend on the flaws of neutron multiplicity sorting. The photoneutron yield cross section is split into partial cross sections using the combined model of photonuclear reactions based on semimicroscopic description of the photoabsorption process and neutron evaporation via the Hauser-Feshbach mechanism and pre-equilibrium exciton model taking into account deformation and isospin effects for medium and heavy nuclei [7–9].

The evaluated partial reaction cross sections

$$\sigma^{\text{eval}}(\gamma, in) = F_i^{\text{theor}} \times \sigma^{\text{exp}}(\gamma, Sn) \quad (3)$$

are determined using the theoretically calculated F_i^{theor} ratios. In the present work this method is used for evaluation of partial and total photoneutron reaction cross sections on the ^{94}Zr isotope.

II. ANALYSIS OF THE RELIABILITY OF THE EXPERIMENTAL DATA USING THE NEUTRON MULTIPLICITY TRANSITIONAL FUNCTIONS F_i

Dobavit' pro dannye. (1) Istochnik. (2) Pochemu

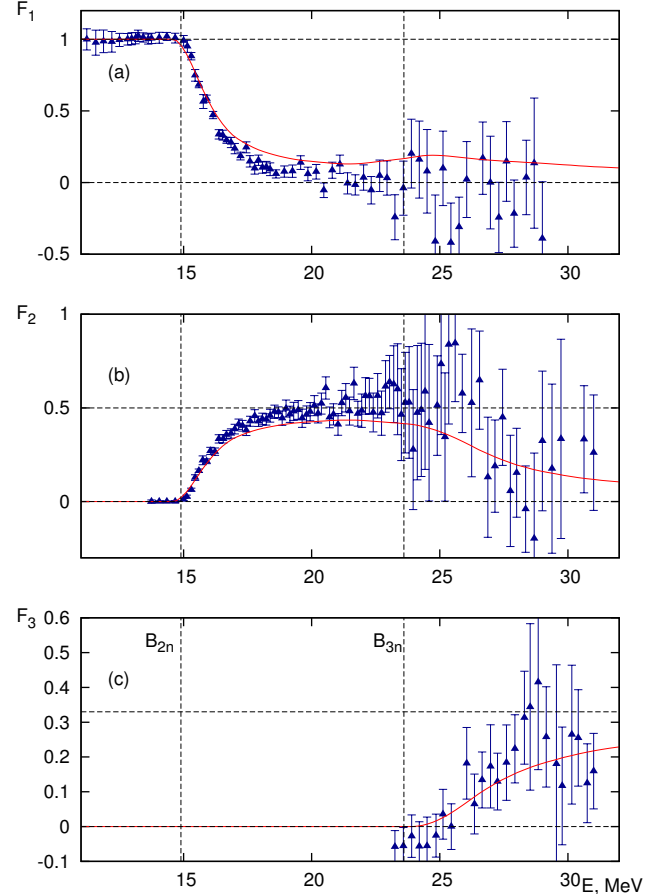


Figure 1. Comparison (from top to bottom: a, b, c for $i = 1, 2, 3$) of the neutron multiplicity transitional functions F_i^{exp} obtained from the experimental data (triangles, [10]) with the F_i^{theor} functions calculated using the theoretical calculations [7–9] for ^{94}Zr .

imenno eti secheniya.

The disagreement of the experimental data and the reliability criteria is described by Fig. 1. The figure shows a comparison of the energy dependencies of the neutron multiplicity transitional functions F_i^{theor} , calculated using the combined model [7–9] (solid lines), with the respective F_i^{exp} values, obtained using the experimental data [10] (triangles with error bars).

It is seen from Fig. 1 that:

1. at the energies below the $B_{2n} = 14.9$ MeV threshold of the $(\gamma, 2n)$ reaction only the $(\gamma, 1n)$ reaction is possible, and, hence, $F_1^{\text{theor}} = 1$, $F_2^{\text{theor}} = F_3^{\text{theor}} = 0$;

- between the B_{2n} and the $B_{3n} = 23.6$ MeV energy thresholds the value of the F_1^{theor} function decreases due to the competition between $\sigma(\gamma, 1n)$ and $\sigma(\gamma, 2n)$, and F_2^{theor} approaches its theoretical limit 0.50;
- behind the B_{3n} reaction threshold F_2^{theor} decreases due to availability of the $(\gamma, 3n)$ reaction channel.

It is also seen from Fig. 1 that there are noticeable differences in the energy dependences of the theoretical and experimental functions F_i :

- at energies greater than 22.2 MeV there are physically unallowed negative values of F_1^{exp} ; it is clear from the comparison of the area of the region of these values under the $F_1^{\text{exp}}(E)$ curve

$$\int_{22.2}^{29.0} F_1^{\text{exp}}(E) dE = -0.55 \pm 0.26 \text{ MeV} \quad (4)$$

with the integrated cross section of the $(\gamma, 1n)$ reaction in the same energy range

$$\int_{22.2}^{29.0} \sigma^{\text{exp}}(E) dE = -19.05 \pm 14.94 \text{ MeV} \cdot \text{mb} \quad (5)$$

that the negative datapoints are statistically meaningful and, thus, the experimental $(\gamma, 1n)$ cross section needs to be corrected in this energy region;

- in the energy range 20.3—26.0 MeV there are F_2^{exp} values exceeding the 0.50 limit; the area under the $F_2(E)$ curve

$$\int_{20.3}^{26.0} F_2(E) dE \quad (6)$$

is 3.20 ± 0.38 MeV for the experimental data [10], and 2.30 ± 0.08 MeV for the theoretical calculation, while according to (1) the maximum allowed value is 2.84 – *otkuda?*; the significant excess of the upper limit of the F_2^{exp} value implies that the $(\gamma, 2n)$ cross section is inconsistent with experimental $\sigma(\gamma, 1n)$ and $\sigma(\gamma, 3n)$ in this energy region; it should be noted that the F_2^{exp} mostly increases in the considered energy interval, though behind the $B_{3n} = 23.6$ MeV threshold a decrease is expected;

- in the energy range below 20.3 MeV there are noticeable disagreements between the F_1^{theor} and F_1^{exp} values, as well as between F_2^{theor} and F_2^{exp} ;
- in the energy range behind 26.5 MeV there are noticeable disagreements between the F_2^{theor} and F_2^{exp} values, as well as between F_3^{theor} and F_3^{exp} .

The most likely reason for the observed discrepancies is that some of the detected neutrons were assigned to wrong reaction channels based on their kinetic energies, that is, the experimental neutron multiplicity sorting was performed incorrectly.

III. EVALUATED CROSS SECTIONS OF PARTIAL PHOTONEUTRON REACTIONS ON THE ^{94}Zr ISOTOPE

As it has been noted above, evaluation of the partial reaction cross sections with the aim of getting rid of the deficiencies of the neutron multiplicity sorting, is based on the corresponding ratios of the theoretical model [7–9], which are used to decompose (2) into reaction channels with different numbers of outgoing neutrons. Prior to the evaluation of the partial reaction cross sections it is important to make sure that the experimental and theoretical neutron yield cross sections (γ, Sn) agree with each other.

In order to match with the experimental data the theoretically calculated photoneutron yield cross section on ^{94}Zr required additional correction by shifting towards greater energies by 0.02 MeV and multiplication by 0.85. The corresponding calculations are shown in Fig. 2 and in table I. It should be noted that the applied correction resulted in almost complete agreement of energy weighted centers of weight of the cross sections in the energy ranges specified in table I.

The cross sections of the $(\gamma, 1n)$, $(\gamma, 2n)$, $(\gamma, 3n)$, and (γ, tot) processes on the ^{94}Zr nucleus, evaluated using relationships (3), are shown in Fig. 3 along with the experimental cross section of the (γ, Sn) reaction taken from [10]. The corresponding integral cross sections are shown in table II.

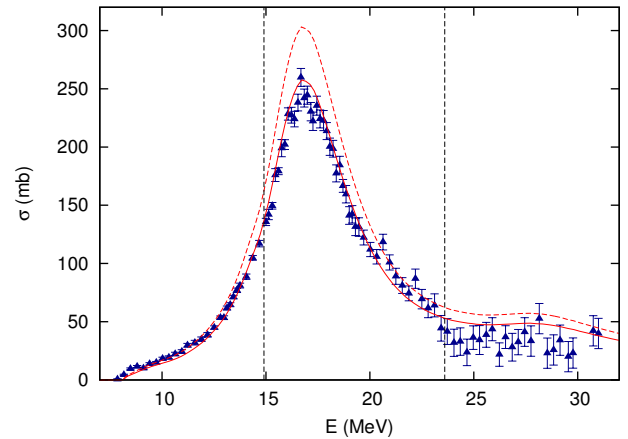


Figure 2. Comparison of the initial (dashed curve) and corrected (solid curve) cross sections of the $^{94}\text{Zr}(\gamma, Sn)$ reaction with the experimental data (triangles, [10]). B_{2n} , B_{3n} denote, respectively, the thresholds of the $(\gamma, 2n)$ and $(\gamma, 3n)$ reactions.

While the experimental and evaluated integrated cross sections of the $(\gamma, 1n)$ reaction are practically the same, (260.6 and 261.8 MeV · mb, respectively), the experimental integrated cross section of the $(\gamma, 1n)$ reaction is 20% less than the evaluation (546.1 and 652.4 MeV · mb, respectively) above the B_{2n} threshold, with the integrated cross section of $(\gamma, 2n)$ being 15% greater (494.5 and 429.0 MeV · mb, respectively).

This overestimation of the experimental $\sigma(\gamma, 2n)$ and underestimation of $\sigma(\gamma, 1n)$ in comparison with the results of evaluation, which is consistently encountered in photonuclear data of 1960–80s, can be explained by the shortcomings of neutron multiplicity sorting based on the

Table I. Integrated cross sections of the $^{94}\text{Zr}(\gamma, \text{Sn})$ reaction

Energy range	$\sigma^{\text{int}}, \text{MeV} \cdot \text{mb}$		
	$E^{\text{int}} = B_{2n} = 15.0 \text{ MeV}$	$E^{\text{int}} = B_{3n} = 23.6 \text{ MeV}$	$E^{\text{int}} = 31.0 \text{ MeV}$
Experimental [10]	299.3 ± 2.7	1545.8 ± 12.3	1779.3 ± 25.2
Theory, initial	333.4 ± 8.8	1820.5 ± 30.3	2228.9 ± 31.6
Theory, corr.	283.1 ± 9.0	1545.5 ± 31.1	1892.2 ± 32.4

Table II. Comparison of integrated cross sections σ^{int} obtained from experimental data [10] and evaluation

Reaction	$\sigma^{\text{int}}, \text{MeV} \cdot \text{mb}$	
	Evaluation	Experimental data
$E^{\text{int}} = B_{2n} = 15.0 \text{ MeV}$		
$(\gamma, \text{Sn})^*$	$282.8 \pm 9.3^*$	299.3 ± 2.7
(γ, tot)	296.5 ± 11.6	298.6 ± 2.7
$(\gamma, 1n)$	295.0 ± 9.9	300.7 ± 2.8
$E^{\text{int}} = B_{3n} = 23.6 \text{ MeV}$		
$(\gamma, \text{Sn})^*$	$1545.3 \pm 32.0^*$	1545.5 ± 12.3
(γ, tot)	1115.2 ± 28.6	1049.9 ± 8.1
$(\gamma, 1n)$	682.2 ± 16.6	585.7 ± 11.6
$(\gamma, 2n)$	427.5 ± 13.6	494.5 ± 7.5
$E^{\text{int}} = 31.0 \text{ MeV}$		
$(\gamma, \text{Sn})^*$	$1892.0 \pm 33.4^*$	1779.3 ± 25.2
(γ, tot)	1237.7 ± 33.0	1125.2 ± 13.4
$(\gamma, 1n)$	722.6 ± 17.6	547.0 ± 23.4
$(\gamma, 2n)$	488.4 ± 15.7	577.2 ± 18.5
$(\gamma, 3n)$	25.1 ± 3.9	31.2 ± 8.3

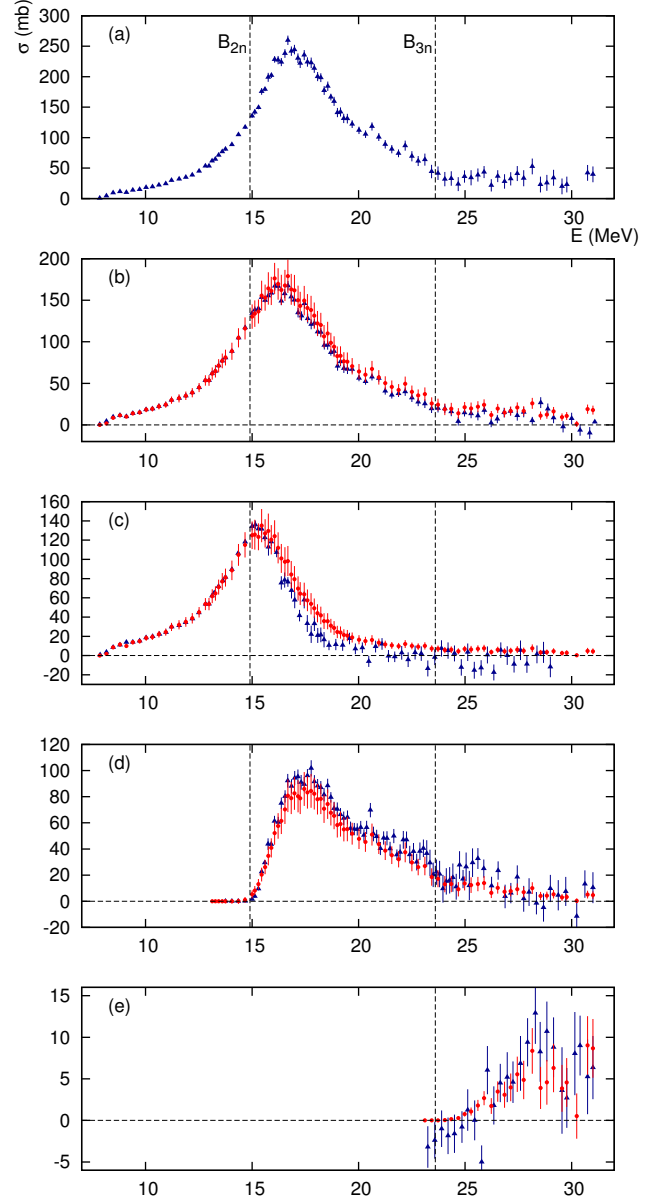
*) Initial cross section [10].

detected kinetic energy. Two important factors were not considered in these measurements: the ambiguity of the relationship between the neutron's multiplicity and kinetic energy and the contribution of the reaction channels with outgoing protons.

When the photon energy increases in the GDR region the shape of the neutron energy spectrum changes only slightly, with the main contribution coming from the neutron with kinetic energies about 1 MeV. It has been shown in [4] on the example of the ^{181}Ta isotope.

The reaction specified as $(\gamma, 1n)$ in [10] is in fact a sum $(\gamma, 1n) + (\gamma, 1n1p)$. Since the $(\gamma, 1n1p)$ on ^{94}Zr has a low energy threshold $B_{np} = 17.8 \text{ MeV}$ and its cross section is of the same order as the cross section of $(\gamma, 2n)$ [7–9], the distribution of the excitation energy between the neutron and the proton in $(\gamma, 1n1p)$ has to be approximately the same as between the two neutrons in $(\gamma, 2n)$. However, the neutron from $(\gamma, 1n1p)$ is multiplicity 1, and the multiplicity of the neutrons in $(\gamma, 2n)$ is 2, which introduces uncertainty in the neutron multiplicity separation procedure based on measuring the kinetic energy used in [10], and makes it not entirely based: the neutrons from the “1n” and “2n” channels entangle with each other and (low energy neutron from $(\gamma, 1n1p)$ are unfoundedly identified as coming from the $(\gamma, 2n)$ reaction instead of $(\gamma, 1n)$).

It should be noted that in the range of energies higher than $B_{3n} = 23.6 \text{ MeV}$ (table II the experimental integrated

Figure 3. Comparison of the evaluated (dots) and experimental ([10], triangles) cross sections of the total and partial photoneutron reactions on ^{94}Zr : (a) $\sigma(\gamma, \text{Sn})$; (b) $\sigma(\gamma, \text{tot})$; (c) $\sigma(\gamma, 1n)$; (d) $\sigma(\gamma, 2n)$; (e) $\sigma(\gamma, 3n)$.

cross section of $(\gamma, 3n)$ is already 60% less than the evaluated value (434.7 vs. 694.9 $\text{MeV} \cdot \text{mb}$), 23% greater for the $(\gamma, 2n)$ reaction (662.6 vs. 539.4 $\text{MeV} \cdot \text{mb}$), and 52% greater for the $(\gamma, 3n)$ reaction (85.4 vs. 56.1 $\text{MeV} \cdot \text{mb}$). This probably means that the errors due to erroneous separation of multiplicity 1 and 3 neutrons, and also separa-

tion multiplicity 2 and 3 neutrons are added to the uncertainties from erroneous separation of multiplicity 1 and 2 neutrons.

IV. CONCLUSIONS

The experimentally measured cross sections of partial photoneutron reactions (γ , 1n), (γ , 2n), and (γ , 3n) on the ^{94}Zr isotope [10], obtained using the neutron multiplicity sorting technique, contain considerable systematic uncertainties and do not satisfy the proposed criteria of reliability. These uncertainties are due to unfounded assignment of the detected neutrons to the “1n”, “2n”, and “3n” channels, which is based on the similarity of the kinetic energies and lack of detection of the proton channels.

The cross sections of the partial reactions (γ , 1n), (γ , 2n), and (γ , 3n) and the total photoneutron reaction (γ , tot) evaluated for ^{94}Zr using the approach (3) are free from the discussed systematic uncertainties. As was shown for partial photoneutron reaction cross sections obtained for ^{181}Ta [4], evaluated data disagree noticeably with data obtained photoneutron multiplicity sorting but agree with data of alternative measurements using induced activity [4, 11].

The work was performed at the Department of nuclear interactions and processes of the Skobeltsyn Institute of Nuclear Physics and partially supported by the RFBR grant No. 13-02-00124. The authors wish to express gratitude to M. A. Makarov for discussions and help in obtaining and representing data.

-
- [1] V. V. Varlamov, B. S. Ishkhanov, V. N. Orlin, V. A. Chetvertkova, *Bull. Russ. Acad. Sci. Phys.* **74**, 833 (2010).
 - [2] V. V. Varlamov, B. S. Ishkhanov, V. N. Orlin, S. Yu. Troschiev, *Bull. Russ. Acad. Sci. Phys.* **74**, 842 (2010).
 - [3] V. V. Varlamov, V. N. Orlin, N. N. Peskov, T. S. Polevich, SINP MSU preprint #2012-1/879, (SINP MSU, Moscow, 2012) [in Russian].
 - [4] B. S. Ishkhanov, V. N. Orlin, S. Yu. Troschiev, *Phys. At. Nucl.* **75**, 353 (2012).
 - [5] V. V. Varlamov, B. S. Ishkhanov, V. N. Orlin, *Phys. At. Nucl.* **75**, 1339 (2012).
 - [6] V. V. Varlamov, B. S. Ishkhanov, V. N. Orlin, N. N. Peskov, K. A. Stopani, *Phys. At. Nucl.* **77**, 1369 (2014).
 - [7] B. S. Ishkhanov, V. N. Orlin, *Phys. Part. Nucl.* **39**, 232 (2007).
 - [8] B. S. Ishkhanov, V. N. Orlin, *Phys. At. Nucl.* **71**, 493 (2008).
 - [9] B. S. Ishkhanov, V. N. Orlin, K. A. Stopani, and V. V. Varlamov, in *The Universe Evolution: Astrophysical and Nuclear Aspects*. Ed. by I. Strakovsky and L. Blokhintsev, (Nova Science Publishers, New York, 2013), p. 113.
 - [10] B. L. Berman, J. T. Caldwell, R. R. Harvey, *et al.*, *Phys. Rev.* **162**, 1098 (1967).
 - [11] V. V. Varlamov, B. S. Ishkhanov, V. N. Orlin, K. A. Stopani, *Eur. Phys. J. A* **50**, 114 (2014).